

# Lawrence Berkeley National Laboratory

## LBL Publications

### Title

Improving aluminum particle reactivity by annealing and quenching treatments:  
Synchrotron X-ray diffraction analysis of strain

### Permalink

<https://escholarship.org/uc/item/7475708k>

### Authors

McCollum, Jena  
Pantoya, Michelle L  
Tamura, Nobumichi

### Publication Date

2016

### DOI

10.1016/j.actamat.2015.10.025

Peer reviewed

Elsevier Editorial System(tm) for Acta Materialia  
Manuscript Draft

Manuscript Number:

Title: Improving Aluminum Particle Reactivity by Annealing and Quenching Treatments: Synchrotron X-ray Diffraction Analysis of Strain

Article Type: Full Length Article

Keywords: Aluminum, dilatational strain, mechanical properties, reactivity, annealing, quenching, synchrotron XRD, energetic materials

Corresponding Author: Prof. Michelle Pantoya, PhD

Corresponding Author's Institution: Texas Tech University

First Author: Jena M McCollum

Order of Authors: Jena M McCollum; Michelle Pantoya, PhD; Nobumichi Tamura, PhD

Abstract: In bulk material processing, annealing and quenching metals such as aluminum (Al) can relieve residual stress and improve mechanical properties. On a single particle level, affecting mechanical properties may also affect Al particle reactivity. This study examines the effect of annealing and quenching on the strain of Al particles and the corresponding reactivity of aluminum and copper oxide (CuO) composites. Micron-sized Al particles were annealed and quenched according to treatments designed to affect Al mechanical properties. Synchrotron X-ray diffraction (XRD) analysis of the particles reveals the thermal treatment increased the dilatational strain of the aluminum-core, alumina-shell particles. Flame propagation experiments also show thermal treatments effect reactivity when combined with CuO. An effective annealing/quenching treatment for increasing aluminum reactivity was identified. These results show that altering the mechanical properties of Al particles affects their reactivity.

Suggested Reviewers: Emily Hunt PhD  
Professor, Engineering, West Texas A&M University  
ehunt@wtamu.edu  
Expertise in aluminum combustion

Keerti Kappagantula PhD  
Professor, Ohio University  
kappagan@ohio.edu  
Expertise in energetic materials

Eric Vogel PhD  
Professor, Materials Science & Engineering, Georgia Tech  
eric.vogel@mse.gtech.edu  
Expertise in metals

Zuhir Munir  
Professor, Materials Science & Engineering, UC Davis  
zamunir@ucdavis.edu

Expertise in metals and combustion



TEXAS TECH UNIVERSITY

Department of Mechanical Engineering

June 16, 2015

Re: Manuscript for publication consideration in *Acta Materialia*

Dear Dr. Mahajan,

Please find our manuscript entitled “Improving Aluminum Particle Reactivity by Annealing and Quenching Treatments: Synchrotron X-ray Diffraction Analysis of Strain,” submitted for publication consideration in *Acta Materialia*. We have not submitted this article elsewhere at any time. Support for this project was provided by a grant from the Army Research Office.

This manuscript focuses on synchrotron x-ray diffraction analysis of aluminum particles that have been treated to improve their mechanical properties. The aluminum is then examined for its reactivity with a metal oxide to show the relationship between material processing and the mechanical properties of the metal then extend this understanding towards application for energy generation technologies. We felt this combination of in-depth analysis of the material property of strain based on annealing and quenching processing of a metal powder and its application to reactivity were the perfect combination of mechanical and functional behavior appropriate for *Acta Materialia*.

Thank you for considering our manuscript.

Sincerely,

Prof. Michelle Pantoya, Ph.D.  
J. W. Wright Regents Endowed Chair Professor  
2703 7<sup>th</sup> Street  
Mechanical Engineering Department  
Texas Tech University  
Lubbock, TX 79409-1021  
Phone: 806-834-3733  
Mobile: 806-438-8671  
Email: [michelle.pantoya@ttu.edu](mailto:michelle.pantoya@ttu.edu)

1  
2  
3  
4  
5  
6  
7  
8  
9  
10  
11  
12  
13  
14  
15  
16  
17  
18  
19  
20  
21  
22  
23  
24  
25  
26  
27  
28  
29  
30  
31  
32  
33  
34  
35  
36  
37  
38  
39  
40  
41  
42  
43  
44  
45  
46  
47  
48  
49  
50  
51  
52  
53  
54  
55  
56  
57  
58  
59  
60  
61  
62  
63  
64  
65

# Improving Aluminum Particle Reactivity by Annealing and Quenching Treatments: Synchrotron X-ray Diffraction Analysis of Strain

*Jena McCollum and Michelle Pantoya*

*Mechanical Engineering, Texas Tech University, Lubbock, TX 79409*

*Nobumichi Tamura*

*Advanced Light Source, Lawrence Berkeley National Laboratory, Berkeley, CA 94720*

## **Abstract**

In bulk material processing, annealing and quenching metals such as aluminum (Al) can relieve residual stress and improve mechanical properties. On a single particle level, affecting mechanical properties may also affect Al particle reactivity. This study examines the effect of annealing and quenching on the strain of Al particles and the corresponding reactivity of aluminum and copper oxide (CuO) composites. Micron-sized Al particles were annealed and quenched according to treatments designed to affect Al mechanical properties. Synchrotron X-ray diffraction (XRD) analysis of the particles reveals the thermal treatment increased the dilatational strain of the aluminum-core, alumina-shell particles. Flame propagation experiments also show thermal treatments effect reactivity when combined with CuO. An effective annealing/quenching treatment for increasing aluminum reactivity was identified. These results show that altering the mechanical properties of Al particles affects their reactivity.

## **Key Words**

Aluminum, dilatational strain, mechanical properties, reactivity, annealing, quenching, synchrotron XRD, energetic materials

## Introduction

Composite energetic materials consist of a metallic fuel (i.e., aluminum (Al)) and a metal oxide (i.e., copper oxide (CuO)). These composites are widely studied due to their high energy densities and heats of combustion. A main goal of much published research studying aluminum combustion is to understand and improve particle reactivity. Towards this end, many have proposed new Al synthesis strategies: such as altering the native aluminum oxide ( $\text{Al}_2\text{O}_3$ ) coating with another passivating agent such as alkenes[1] or applying self-assembled monolayers (SAM) to the particle surface[2]. Various explanations for Al oxidation mechanisms have also been proposed, each strongly tied to the ignition mechanism and heating rate[3]–[11]. All theories share a common theme for mass transport of fuel and oxidizer, but differ in how that diffusion is achieved (i.e., via (a) dispersion[3], [4], (b) phase changes in the polymorphous passivation shell[5]–[7], (c) reactive sintering[8], (d) pressure gradient driven processes[9], [10], and (e) induced electric field influences[11]). This article will not directly deal with any particular reaction mechanism, but rather investigate the influence of a new parameter, mechanical strain, which has only recently been considered in the study of Al oxidation[3], [4], [12], [13].

A typical aluminum particle consists of an aluminum core passivated by an alumina shell as seen in Fig. 1. Residual stress within an aluminum particle is induced during production. These are thermally induced stresses that are generated during the cooling stage. Stress builds in two stages during particle synthesis: (1) within the aluminum core during cooling and prior to oxide shell formation; and, (2) during alumina shell formation until the core-shell system reaches ambient temperature conditions.

Within the molten aluminum droplet absent of a shell, stress develops as the molten aluminum droplet cools, because external surface layers start to shrink while the core is still hot

1  
2  
3  
4 and free to contract but its contraction is constrained by the external layers that have solidified  
5  
6 and become rigid. In this way, the stress distribution in a naked aluminum particle is tensile in  
7  
8 the core and compressive at the surface. Smaller particles cool at faster rates[14]–[16] and should  
9  
10 manifest larger internal stresses during production.  
11  
12

13  
14 The shell is formed when oxygen is introduced at temperatures below the melting  
15  
16 temperature of aluminum (i.e., < 660 °C[17]) and no higher than 440 °C (i.e., the phase transition  
17  
18 of amorphous to gamma alumina[18]). At this point, another residual stress develops because  
19  
20 there exists a mismatch of thermal expansion coefficients (i.e.,  $a$ , linear coefficient; or,  $b$ ,  
21  
22 volumetric coefficient) between the newly formed alumina shell (i.e.,  $a_{ox} = 5 \times 10^{-6} \text{ K}^{-1}$  and  $b_{ox} = 8$   
23  
24  $\times 10^{-6} \text{ K}^{-1}$ [18]) and aluminum core ( $a_m = 23 \times 10^{-6} \text{ K}^{-1}$  and  $b_m = 69 \times 10^{-6} \text{ K}^{-1}$  [17]). Cooling from  
25  
26 440 °C to ambient will induce shrinkage in the core while the shell remains relatively rigid, i.e.,  
27  
28 there is an order of magnitude difference in expansion coefficients. The internal radius of the  
29  
30 oxide sphere is forced to decrease and stresses arise at the interface of the core-shell.  
31  
32

33  
34 Isothermal stress relief is a common approach to stress relaxation[19]–[21]. This  
35  
36 technique involves the uniform heating of a material to a specified temperature below the  
37  
38 melting temperature, holding at that temperature for a period of time, followed by cooling to  
39  
40 control the re-introduction of desirable thermal stresses. This sequence of steps is referred to as  
41  
42 annealing followed by quenching. Timoshenko and others[19]–[23] explain significant  
43  
44 microstructural changes take place that promote stress relief at about two-thirds the temperature  
45  
46 at which the stresses were formed. In the case of Al particles, the amorphous alumina shell is  
47  
48 formed at roughly 440 °C such that annealing temperatures should at least be 293 °C.  
49  
50

51  
52 Interestingly, Firmansyah et al. examined the stress state of nano-aluminum powder upon  
53  
54  
55  
56  
57  
58  
59  
60  
61  
62  
63  
64  
65

1  
2  
3  
4 continuous heating using a high temperature XRD and found that Al particles experience a zero-  
5 stress state at 300 °C[24].  
6  
7

8  
9 The main mechanism that causes relaxation of locked-in stresses for annealing  
10 temperatures < 400°C is classical diffusional creep. This mechanism enables counterbalancing  
11 regions of tensile and compressive stresses to contract or expand slightly, and thus to  
12 redistribute. This is also a time dependent process and determining the optimum temperature and  
13 duration for annealing and quenching has not previously been investigated for aluminum  
14 particles. Some experimental work on other metals has revealed a relevant conclusion: while the  
15 annealing time is important, creep is a logarithmic process such that most relief is obtained at a  
16 given temperature rapidly[20]. Data presented by Adeyemi et al. for carbon steel suggests  
17 annealing times on the order of 10 minutes should be sufficient to relieve stress[25]. Even for the  
18 annealing temperature of 500°C, 80% of the residual stress is relieved in 5 minutes. Bulk  
19 aluminum alloys have been studied for creep behavior [26]. Prasad et al. studied creep at 87 and  
20 200 °C and found the effects of stress increments and decrements to be different[26]. This is an  
21 important finding because it implies stress variations are significant in the temperature ranges we  
22 are most interested (i.e., < 400 °C).  
23  
24  
25  
26  
27  
28  
29  
30  
31  
32  
33  
34  
35  
36  
37  
38  
39  
40  
41  
42

43 Quenching is another important variable to consider. Evancho et al. showed that slow  
44 cooling may re-introduce thermal stresses that are undesirable (e.g., like the residual stress) and  
45 lead to lower strength[27]. Faster cooling rates may effectively ‘freeze’ the stress state such that  
46 purposefully induced desirable thermal stress do not have time to relax, leading to higher  
47 strength. The hypothesis is: faster cooling rates will produce aluminum particles with optimal  
48 mechanical properties promoting optimal reactivity.  
49  
50  
51  
52  
53  
54  
55  
56  
57  
58  
59  
60  
61  
62  
63  
64  
65



1  
2  
3  
4 Dikici et al. showed preliminary evidence that annealing and quenching Al particles  
5  
6 affects reactivity [13]. They heated Al particles to a prescribed temperature then cooled them to  
7  
8 room temperature and found that some thermal treatments lead to improved flame speeds. Their  
9  
10 powders were allowed to cool at two different rates. The samples that were cooled at 0.06 KPS  
11  
12 (Kelvin per second) showed flame speeds comparable to the untreated samples, but when the  
13  
14 cooling rate was raised to 0.13 KPS, the flame speeds for micron scale Al and molybdenum  
15  
16 trioxide ( $\text{MoO}_3$ ) improved for one case and worsened for the other. More recently, Levitas et al.  
17  
18 extended the work by Dikici et al. by focusing on micron scale Al particles and using a different  
19  
20 metal oxide (i.e., copper oxide ( $\text{CuO}$ ))[12]. They examined flame speeds and showed certain  
21  
22 thermal treatments were consistent with predictions of the melt dispersion mechanism,  
23  
24 effectively expanding the realm of this reaction mechanism towards optimization of micron scale  
25  
26 Al particles [12].  
27  
28  
29  
30  
31

32  
33 The objective of this study is to fundamentally quantify changes in strain associated with  
34  
35 Al particle thermal treatments and examine energy propagation behavior of treated Al particles  
36  
37 combined with CuO. These extensions enable an understanding of how thermal treatment and  
38  
39 mechanical properties couple to influence the reactivity of Al particles with a solid oxidizer.  
40  
41 Improving Al reactivity with a relatively simplistic heat treatment approach may greatly improve  
42  
43 their functional application.  
44  
45  
46  
47

## 48 49 **Experimental**

### 50 51 *Sample Preparation*

52  
53 Aluminum particles were procured from Alfa Aesar (Ward Hill, MA). Their average  
54  
55 diameter was determined using an AccuSizer 780 optical particle size analyzer (Santa Barbara,  
56  
57  
58  
59  
60

1  
2  
3  
4 CA). The Al particles were suspended in filtered water (specifically, 2 mg Al/80 ml water) and  
5  
6  
7 sonicated for 60 minutes in cycles of 10 seconds on, 10 seconds off in order to avoid heating.  
8  
9 The sample was then pulled via a syringe pump for analysis. Particle length (diameter) is  
10  
11 calculated and plotted as a count-based measurement. The plot for the untreated Al is shown in  
12  
13 Fig. 2a and the size data is given in Fig. 2e. The oxide thickness used for purity calculations was  
14  
15 estimated at 3 nm (i.e., >1% oxide concentration, see Fig. 1). The untreated Al particles have an  
16  
17 average diameter of 5 microns.  
18  
19

20  
21 Aluminum particles (200 mg) were loaded into ceramic trays and subjected to various  
22  
23 annealing temperatures and quenched to room temperature. This process used a Neytech Qex  
24  
25 vacuum oven (Torrance, CA). This is a programmable oven, such that the powder was annealed  
26  
27 to 100, 200 or 300°C at a controlled rate of 10 Kelvin per minute (KPM), held at the prescribed  
28  
29 temperature for 15 minutes then removed from the oven and quenched via refrigeration to room  
30  
31 temperature for 15 minutes then removed from the oven and quenched via refrigeration to room  
32  
33 temperature in air at standard pressure. Powder temperature was monitored using an InstruNet  
34  
35 Direct to Sensor system (Charlestown, MA) and Type K thermocouples from Omega  
36  
37 Engineering (Stamford, CT). Aluminum temperature was monitored for each thermal cycle and  
38  
39 Fig. 3 shows the temperature response as a function of time.  
40  
41

42  
43 For the natural convection conditions that exist in these experiments, materials cool  
44  
45 according to a lump capacitance model. The quenching rate is an exponential function of time as  
46  
47 shown in Eq. (1). The temperature evolution reduces exponentially and experimental results are  
48  
49 approximated by Eq. (1).  
50  
51

$$52 \quad T = T_a + (T_0 - T_a) \exp(-At) \text{ with } A = 0.0078 \text{ s}^{-1} \quad (1)$$

53  
54  
55 In Eq. (1)  $T_a$  is ambient temperature,  $T_0$  is annealing temperature,  $t$  is time and  $A$  is  
56  
57 determined by examining the exponential plots of the cooling curves and identifying the  
58  
59  
60  
61  
62  
63  
64  
65

1  
2  
3  
4 coefficient. An average quenching rate ranges from 0.13 to 0.38 KPS depending on annealing  
5  
6 temperature.  
7

8  
9 The Al particles were then mixed with 50 nm average particle diameter spherical CuO  
10 particles (Sigma Aldrich (St. Louis, MO)) to an equivalence ratio of 1.2 (i.e., slightly fuel rich).  
11 The mixing process is well documented[28]–[30] but will be summarized here. The dry powders  
12  
13 were weighed and suspended in hexane and mixed using a Misonix Sonicator 3000 probe for 2  
14  
15 minutes. The solution is poured into a Pyrex dish and hexane evaporated in a fume hood for 24  
16  
17 hours. The dry powders were retrieved and sieved to break up large agglomerations.  
18  
19  
20  
21  
22

23 The powder is carefully loaded into 3 mm inner diameter, 8 mm outer diameter, 10 cm  
24 long quartz tubes containing 850 mg of powder each. The theoretical maximum density (TMD)  
25 of the loose powder is determined by a weighted average of the bulk densities of Al (2.7 g/cm<sup>3</sup>),  
26 Al<sub>2</sub>O<sub>3</sub> (3.95 g/cm<sup>3</sup>), and CuO (6.31 g/cm<sup>3</sup>). This is calculated using Eq. (2) where  $M$  is the  
27 percent mass of reactant  $i$  and  $\rho$  is the density for each reactant.  
28  
29  
30  
31  
32  
33  
34

$$TMD = \frac{1}{\sum_i M_i \frac{1}{\rho_i}} \quad (2)$$

35  
36  
37  
38  
39  
40 The calculated TMD is 5.46 g/cm<sup>3</sup> and the bulk density is 1.04 g/cm<sup>3</sup> such that tubes  
41 were loaded to 19% TMD.  
42  
43  
44  
45

### 46 *Strain Measurements*

47  
48  
49  
50 X-Ray Diffraction (XRD) experiments were performed at the Advanced Light Source on  
51 beamline 12.3.2 using a micron focused synchrotron x-ray beam. This is a unique facility that  
52 allows measurement of micron-scale samples. Aluminum powder samples were spread over  
53 glass slides and scanned under the x-ray beam (either polychromatic or monochromatic) while a  
54  
55 diffraction pattern was collected at each step using a DECTRIS Pilatus 1 M detector. The  
56  
57  
58  
59  
60  
61  
62  
63  
64  
65

1  
2  
3  
4 measured relative small shifts in the reflection positions in the Laue pattern provides the  
5  
6 deviatoric strain tensor of the material while the measurement of the energy of one reflection  
7  
8 provides the dilatational component. Data were processed using XMAS software[31]. The  
9  
10 beamline experimental setup and capabilities have been described elsewhere[32].  
11  
12

### 13 14 ***Flame Speed Measurements***

15  
16 Figure 4 illustrates a typical powder filled tube arrangement for measuring flame speed as  
17  
18 well as representative still frame images of flame propagation. The apparatus and procedure are  
19  
20 described in more detail elsewhere[13] but summarized here. Both ends of the tube were sealed  
21  
22 with one side securing a length of nickel-chromium wire for ignition. Five experiments per  
23  
24 annealing temperature were performed to establish repeatability. Each tube was placed inside a  
25  
26 blast chamber for ignition and flame propagation experiments. The powders were ignited and  
27  
28 flame propagation was observed through a viewing window in the chamber (as seen in Fig. 5).  
29  
30  
31 The reaction was recorded with a Phantom v7 (Vision Research, Wayne, NJ) high speed camera  
32  
33 at a rate of 29,000 frames per second and 512 x 128 resolution. The camera was aligned  
34  
35 perpendicular to the direction of flame propagation. Flame speed was determined by tracking  
36  
37 the flame front through a referenced time and distance using the Vision Research Software. The  
38  
39 resolution of the flame speed for this diagnostic is 0.1 m/s. The largest source of uncertainty in  
40  
41 the measurement is due to repeatability and is shown for each data set in the results.  
42  
43  
44  
45  
46  
47  
48  
49  
50

### 51 **Results**

52  
53 Further particle size analyses were performed for each Al sample after thermal treatment.  
54  
55 Figures 2b-d show the plots for Al particle sizing and the average particle diameter and  
56  
57  
58  
59  
60  
61  
62  
63  
64  
65

1  
2  
3  
4 distribution is given in Fig. 2e. This data shows that the thermal treatments did not result in  
5  
6 sintering or agglomerations because the average diameter remains consistent (about 5.9  $\mu\text{m}$ ).  
7  
8

9 Figure 6 shows results of dilatational strain (i.e. change in volume) distribution  
10  
11 measurements of aluminum particles that were (a) untreated and annealed to (b) 100°C, (c)  
12  
13 200°C and (d) 300°C. Table 1 presents the count based averages for dilatational strain for each  
14  
15 annealing temperature. The average strain for the samples annealed to 100 and 200 °C fall  
16  
17 within the resolution of the machine ( $2 \times 10^{-5}$ ), so their percent increase was negligible. However,  
18  
19 the aluminum particles annealed to 300°C and cooled to room temperature showed a significant  
20  
21 dilatational strain increase from the baseline Al particles (i.e. 660%). It is noted that these  
22  
23 measurements are of the aluminum core because the alumina shell is too thin (i.e., less than 5  
24  
25 nm) to resolve volume based strain measurements using this approach.  
26  
27  
28  
29  
30

31 Figure 7 shows flame speed as a function of annealing temperature. The samples  
32  
33 annealed to 100°C experience a 2% increase in flame speed from the baseline; and, when  
34  
35 annealed to 200°C flame speed increases by 3%. Once the samples are annealed to 300°C, they  
36  
37 experience a 23% increase in flame speed. This is a significant increase in reactivity for the  
38  
39 composite annealed to 300°C but not for the other annealing temperatures. These results are also  
40  
41 summarized in Table 1.  
42  
43  
44  
45  
46  
47

## 48 **Discussion**

49

50 Figure 6 shows that compared to the baseline, volumetric strain increases as annealing  
51  
52 temperature increases. According to Fig. 6 and Table 1, average dilatational strain increases by  
53  
54 660% after thermal treatment to 300 °C but is unchanged in the samples annealed to 100 and 200  
55  
56 °C. Diffusional creep resistance occurs in samples when the annealing temperature is below a  
57  
58  
59  
60  
61  
62  
63  
64  
65

1  
2  
3  
4 critical fraction of the melt temperature (i.e.,  $T_m = 660\text{ }^\circ\text{C}$  for Al)[33]. Kitagawa et al.  
5  
6 investigated creep response in bulk Al samples subjected to a variety of temperatures (i.e., from  
7  
8  $0.32T_m$  ( $\sim 27\text{ }^\circ\text{C}$ ) to  $0.55T_m$  ( $\sim 240\text{ }^\circ\text{C}$ )) for different number of thermal treatment cycles. They  
9  
10 were interested to see the average creep rate for each temperature over a variety of thermal  
11  
12 cycles and found that the transition temperature for Al to exhibit creep acceleration is  $0.4T_m$  (i.e.,  
13  
14  $100\text{ }^\circ\text{C}$ ) and the maximum acceleration of creep for Al occurs at about  $0.52T_m$  ( $212\text{ }^\circ\text{C}$ ). Figure 4  
15  
16 shows that the samples annealed to  $100$  and  $200\text{ }^\circ\text{C}$  show little response in terms of dilatational  
17  
18 strain, consistent with annealing temperatures below the critical temperature for maximum  
19  
20 acceleration of creep (i.e.,  $212\text{ }^\circ\text{C}$ ). However, once this critical temperature is passed (i.e.,  $300$   
21  
22  $^\circ\text{C}$ ), the Al particles responded with a  $660\%$  increase in dilatational strain. The effect of this  
23  
24 trend is seen in the flame speed results. The Al samples annealed to  $100$  and  $200\text{ }^\circ\text{C}$  showed  
25  
26 little change from the untreated case, but for the  $300\text{ }^\circ\text{C}$  case, flame speeds increased by  $24\%$ .  
27  
28  
29  
30  
31  
32

33  
34 Ultimately, the annealing and quenching treatment effectively increased the overall  
35  
36 strain. It is important to note that at higher annealing temperature or longer annealing times,  
37  
38 particles could experience shell growth and/or oxide phase change. Amorphous alumina begins  
39  
40 to transition to gamma-phase alumina around  $440\text{ }^\circ\text{C}$ , such that annealing beyond this  
41  
42 temperature would affect the shell microstructure, which may also impact reactivity. Also,  
43  
44 annealing to temperatures past  $440\text{ }^\circ\text{C}$  for an extended time ( $60+$  minutes) would result in oxide  
45  
46 layer growth as shown by Gesner et al.[34]. They annealed  $95\text{ nm}$  diameter Al particles to  $480$   
47  
48  $^\circ\text{C}$  for a variety of hold times and saw an increase in oxide shell thickness from  $2.7$  to  $8.3\text{ nm}$   
49  
50 when held for  $150$  minutes but negligible shell growth for times applied in this study (and in this  
51  
52 study annealing temperatures did not exceed  $300\text{ }^\circ\text{C}$ ).  
53  
54  
55  
56  
57  
58  
59  
60  
61  
62  
63  
64  
65

1  
2  
3  
4 The thermal treatment is purposefully designed to relax residual stresses by annealing  
5  
6 then reintroduce desirable stresses by quenching. While thermal treatments are relatively  
7  
8 established for bulk metal processing, manipulation of mechanical properties for particles that  
9  
10 consist of a core-shell structure are not well understood. In this study, results for thermal  
11  
12 treatment of particles appear to be consistent with theory for bulk metals. The benefit of thermal  
13  
14 treatment from Figs. 6 and 7 is that the 300 °C annealed and quenched Al powders now exhibit  
15  
16 higher strain that also correlates with higher macroscopic energy propagation.  
17  
18  
19  
20  
21  
22

## 23 **Conclusion**

24  
25  
26  
27 This study examines the effect of aluminum powder annealing and quenching treatments  
28  
29 on strain in aluminum particles and corresponding reactivity. Micron-sized aluminum powder  
30  
31 was annealed and quenched according to treatments designed to affect mechanical properties.  
32  
33 Synchrotron X-ray diffraction (XRD) analysis of the particles reveals annealing increased the  
34  
35 dilatational strain of the Al particles. Diffusional creep is the primary mechanism affecting strain  
36  
37 and for powder annealed to 300 °C, 660 % increase in dilatational strain was observed.  
38  
39 However, annealing to 100 or 200 °C showed no significant increase in dilatational strain.  
40  
41 Treated Al powder was then mixed with CuO to assess reactivity. Flame speed measurements  
42  
43 similarly showed the 300°C annealed sample produced the highest flame speed. These results  
44  
45 reveal that altering the mechanical properties of aluminum particles affects their reactivity,  
46  
47 particularly when combined with a solid oxidizer.  
48  
49  
50  
51  
52  
53  
54  
55  
56  
57  
58  
59  
60  
61  
62  
63  
64  
65

1  
2  
3  
4 **Acknowledgments**  
5  
6  
7

8 The authors acknowledge support from ARO under contract W911NF-11-1-0439 and  
9 encouragement from our program manager, Dr. Ralph Anthenien. The authors are grateful for  
10 partial support from ONR under contract (N00014-12-1-0525) managed by Dr. C. Bedford. The  
11 Advanced Light Source is supported by the Director, Office of Science, Office of Basic Energy  
12 Sciences, Materials Sciences Division, of the U.S. Department of Energy under Contract No.  
13 DE-AC02-05CH11231 at Lawrence Berkeley National Laboratory and University of California,  
14 Berkeley, California.  
15

16  
17 **References**  
18  
19  
20

- 21 [1] S. W. Chung, E. A. Guliants, D. W. Bunker, C.E., Hammerstroem, W. Douglas, Y. Deng,  
22 M. A. Burgers, P. A. Jelliss, and S. W. Buckner, Capping and Passivation of Aluminum  
23 Nanoparticles Using Alkyl-Substituted Epoxides, *Langmuir*. 25 (2009) 8883–8887.  
24  
25 [2] K. S. Kappagantula, M. L. Pantoya, and J. Horn, Effect of surface coatings on aluminum  
26 fuel particles toward nanocomposite combustion, *Surf. Coatings Technol.* 237 (2013)  
27 456–459.  
28  
29 [3] V. I. Levitas, B. W. Asay, S. F. Son, and M. Pantoya, Melt dispersion mechanism for fast  
30 reaction of nanothermites, *Appl. Phys. Lett.* 89 (2006) 071909.  
31  
32 [4] V. I. Levitas, B. W. Asay, S. F. Son, and M. Pantoya, Mechanochemical mechanism for  
33 fast reaction of metastable intermolecular composites based on dispersion of liquid metal,  
34 *J. Appl. Phys.* 101 (2007) 083524.  
35  
36 [5] M. A. Trunov, M. Schoenitz, and E. L. Dreizin, Effect of polymorphic phase  
37 transformations in the alumina layer on ignition of aluminum particles, *Combust. Theory*  
38 *Model*. 10 (2006) 603–623.  
39  
40 [6] E. L. Dreizin, On the mechanism of asymmetric aluminum particle combustion, *Combust.*  
41 *Flame*. 117 (1999) 841–850.  
42  
43 [7] M. a Trunov, S. M. Umbrajkar, M. Schoenitz, J. T. Mang, and E. L. Dreizin, Oxidation  
44 and melting of aluminum nanopowders., *J. Phys. Chem. B*. 110 (2006) 13094–9.  
45  
46 [8] K. T. Sullivan, N. W. Piekielek, C. Wu, S. Chowdhury, S. T. Kelly, T. C. Hufnagel, K.  
47 Fezzaa, and M. R. Zachariah, Reactive sintering: An important component in the  
48 combustion of nanocomposite thermites, *Combust. Flame*. 159 (2012) 2–15.  
49  
50 [9] A. Rai, K. Park, L. Zhou, and M. R. Zachariah, Understanding the mechanism of  
51 aluminum nanoparticle oxidation, *Combust. Theory Model*. 10 (2006) 603–623.  
52  
53  
54  
55  
56  
57  
58  
59  
60  
61  
62  
63  
64  
65



- 1  
2  
3  
4 [10] K. Sullivan and M. R. Zachariah, Simultaneous pressure and optical measurements of  
5 nanoaluminum thermites: investigating the reaction mechanism, *J. Propuls. power.* 26  
6 (2010) 467–472.  
7  
8  
9 [11] P. Chakraborty and M. R. Zachariah, Do nanoenergetic particles remain nano-sized during  
10 combustion?, *Combust. Flame.* 161 (2014) 1408–1416.  
11  
12 [12] V. I. Levitas, J. Mccollum, and M. L. Pantoya, Improving micron - scale aluminum core -  
13 shell particles reactivity by pre - stressing, *Sci. Rep. Mdm* (2015) 1–12.  
14  
15 [13] B. Dikici, M. L. Pantoya, and V. Levitas, The effect of pre-heating on flame propagation  
16 in nanocomposite thermites, *Combust. Flame.* 157 (2010) 1581–1585.  
17  
18 [14] B. Zheng, Y. Lin, Y. Zhou, and E. J. Lavernia, Gas Atomization of Amorphous  
19 Aluminum: Part I. Thermal Behavior Calculations, *Met. Mater. Trans. B.* 40 (2009) 768–  
20 778.  
21  
22 [15] B. Zheng, Y. Lin, Y. Zhou, and E. J. Lavernia, Gas Atomization of Amorphous  
23 Aluminum: Part II. Experimental Investigations, *Met. Mater. Trans. B.* 40 (2009) 995–  
24 1004.  
25  
26 [16] S. Ozbilen, A. Unal, and T. Sheppard, Influence of Atomizing Gases on the Oxide-Film  
27 Morphology and Thickness of Aluminum Powders, *Oxid. Met.* 53 (2000) 1–22.  
28  
29 [17] J. E. Hatch, *Aluminum: Properties and Physical Metallurgy*, Ohio, 1984.  
30  
31 [18] H. Dorre and H. Hubner, *Alumina: Processing, Properties and Applications*, Springer,  
32 Berlin, 2011.  
33  
34 [19] J. F. Throop, J. H. Underwood, and G. S. Legar, *Residual Stress and Stress Relaxation.*  
35 Plenum Press, (1971).  
36  
37 [20] M. R. James, *Relaxation of Residual Stresses: An Overview*, *Technol. Appl. Eff.* 1987.  
38  
39 [21] L. W. Crane, *Heat Treatment Methods Media*, *Inst. Met. Tech.* (1979) 1–10.  
40  
41 [22] J. Vilms and D. Kerps, Simple Stress Formula for Multilayered Thin Films on a Thick  
42 Substrate, *J. Appl. Phys.* 53 (1982) 1536–1537.  
43  
44 [23] W. D. Kingery, Factors Affecting Thermal Stress Resistance of Ceramic Materials, *J. Am.*  
45 *Ceram. Soc.* 38 (1955).  
46  
47 [24] D. A. Firmansyah, K. Sullivan, K.-S. Lee, Y. H. Kim, R. Zahaf, M. R. Zachariah, and D.  
48 Lee, Microstructural Behavior of the Alumina Shell and Aluminum Core Before and After  
49 Melting of Aluminum Nanoparticles, *J. Phys. Chem. C.* 116 (2012) 404–411.  
50  
51  
52  
53  
54  
55  
56  
57  
58  
59  
60  
61  
62  
63  
64  
65

- 1  
2  
3  
4 [25] M. B. Adeyemi, G. F. Modlen, and R. A. Stark, Stress Relaxation in Cold Worked Mild  
5 Steel, *Met. Sci.* 17 (1983) 43–47.  
6  
7  
8 [26] Y. V. R. . Prasad, D. H. Sastry, and K. I. Vasu, A Study of Low Temperature Creep in  
9 Aluminum by Change in Stress Experiments: Thermal Activation of Attractive Junctions,  
10 *Met. Sci.* 4 (1970) 69–73.  
11  
12  
13 [27] J. W. Evancho and J. T. Staley, Kinetics of Precipitation in Aluminum Alloys During  
14 Continuous Cooling, *Metall. Trans. A*, vol. 5 (1974) 43–47.  
15  
16 [28] C. a. Crane, M. L. Pantoya, and B. L. Weeks, Investigating the trade-offs of microwave  
17 susceptors in energetic composites: Microwave heating versus combustion performance, *J.*  
18 *Appl. Phys.* 115 (2014) 104-106.  
19  
20  
21 [29] J. Feng, G. Jian, Q. Liu, and M. R. Zachariah, Passivated iodine pentoxide oxidizer for  
22 potential biocidal nanoenergetic applications., *ACS Appl. Mater. Interfaces.* 5 (2013)  
23 8875–8880.  
24  
25  
26 [30] K. Kappagantula, C. Crane, and M. Pantoya, Factors Influencing Temperature Fields  
27 during Combustion Reactions, *Propellants, Explos. Pyrotech.* 39 (2014) 434–443  
28  
29  
30 [31] M. Kunz, N. Tamura, K. Chen, A. A. MacDowell, R. S. Celestre, M. M. Church, and E.  
31 Ustundag, A dedicated superbend X-ray microdiffraction beamline for materials, geo-,  
32 and environmental sciences at the advanced light source., *Rev. Sci. Instrum.* 80 (2009)  
33 035108.  
34  
35  
36 [32] N. Tamura, XMAS: a versatile tool for analyzing synchrotron x-ray microdiffraction data.  
37 Microdiffraction analysis local and near surface hierarchical organization of defects.  
38 London, 2013.  
39  
40  
41 [33] M. Kitagawa, C. E. Jaske, and J. Morrow, Influence of Temperature on Reversed Creep,  
42 American Society for Testing and Materials, 1969, pp. 100–110.  
43  
44  
45 [34] J. Gesner, M. L. Pantoya, and V. I. Levitas, Effect of oxide shell growth on nano-  
46 aluminum thermite propagation rates, *Combust. Flame.* 159 (2012) 3448–3453.  
47  
48  
49  
50  
51  
52  
53  
54  
55  
56  
57  
58  
59  
60  
61  
62  
63  
64  
65

# Improving Aluminum Particle Reactivity by Annealing and Quenching Treatments: Synchrotron X-ray Diffraction Analysis of Strain

*Jena McCollum and Michelle Pantoya*

*Mechanical Engineering, Texas Tech University, Lubbock, TX 79409*

*Nobumichi Tamura*

*Advanced Light Source, Lawrence Berkeley National Laboratory, Berkeley, CA 94720*

## Figures

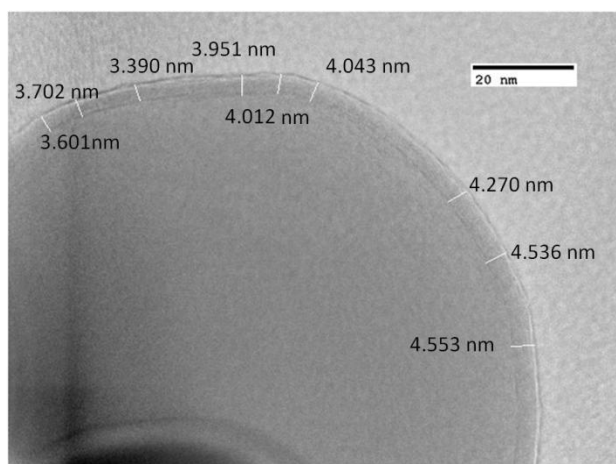
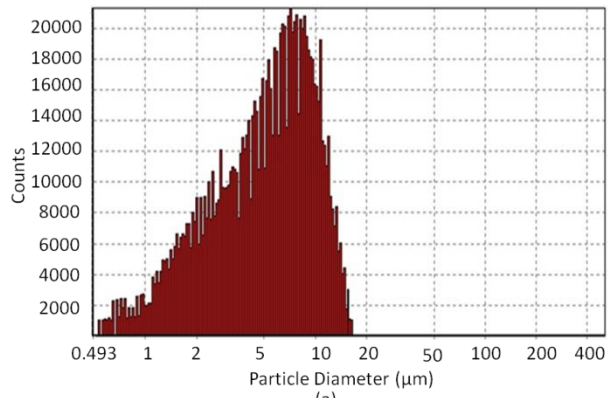
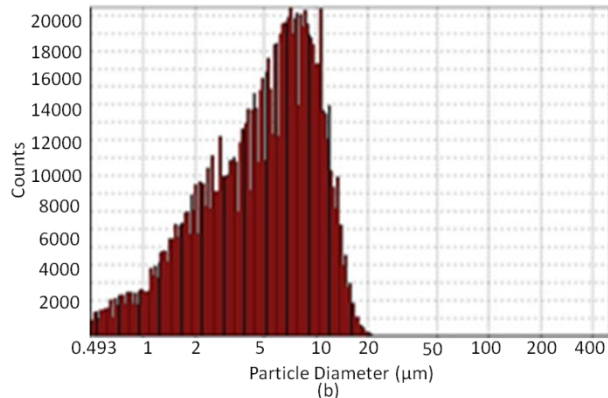


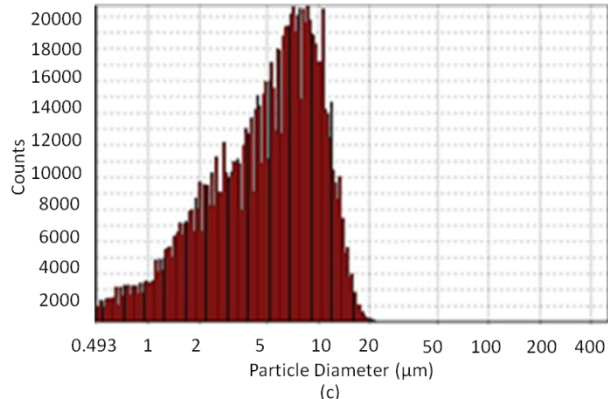
Figure 1. Transmission electron spectroscopy (TEM) image of a nano-scale Al particle to show alumina shell thickness. The average thickness is 4.01 nm. This thickness was used in the purity calculations for micron-scale Al particles (< 1% by mass oxide).



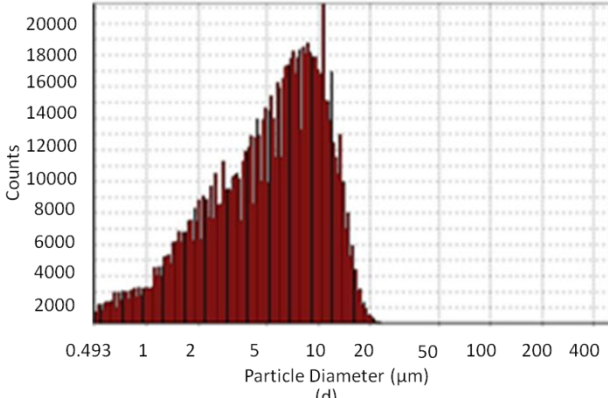
(a)



(b)



(c)



(d)

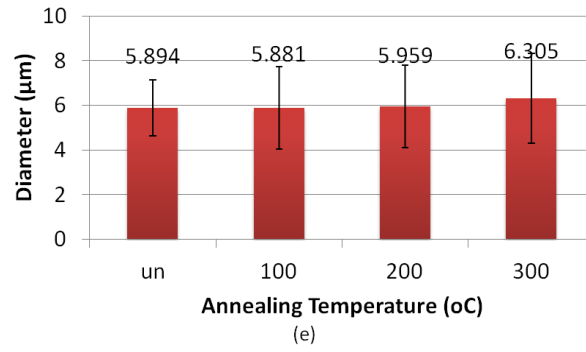


Figure 2. Particle size distribution of (a) untreated Al and Al annealed to (b) 100 °C, (c) 200 °C, (d) 300 °C and (e) average particle diameter with standard deviation for each Al powder sample.

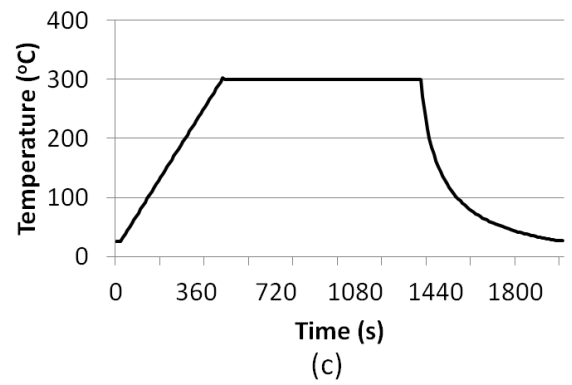
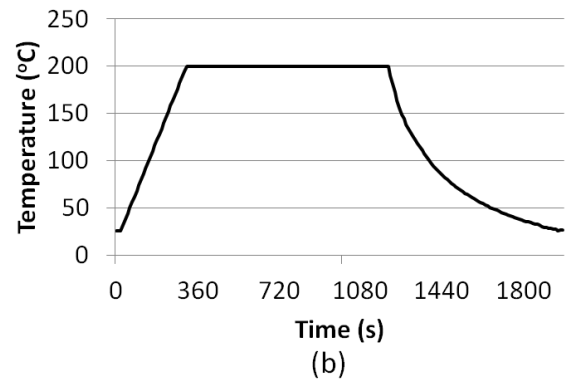
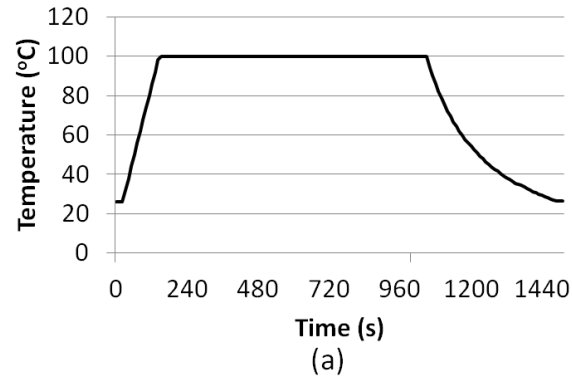


Figure 3. Temperature plots for Al thermal cycles to (a) 100 °C, (b) 200 °C and (c) 300 °C.

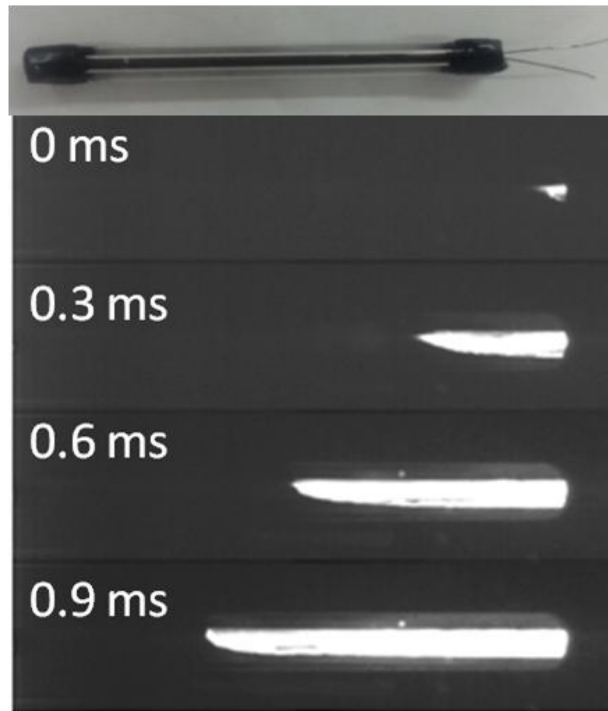


Figure 4: Powder filled quartz tube and representative still frame images time stamped of powder filled quartz tube and flame propagation. Bulk density is 19% theoretical maximum density. Note nichrome wire extruding for left end of the tube.

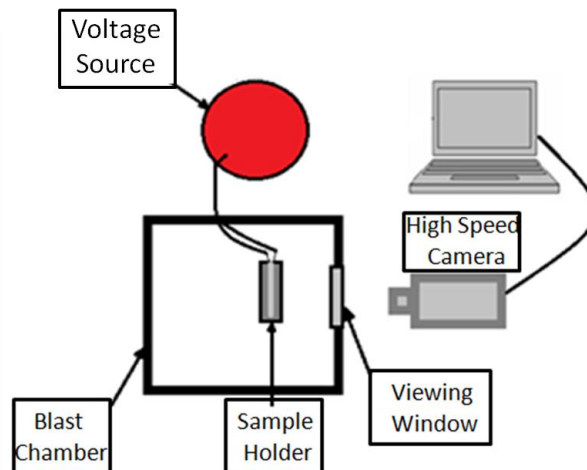


Figure 5. Ignition setup for tracking energy propagation.

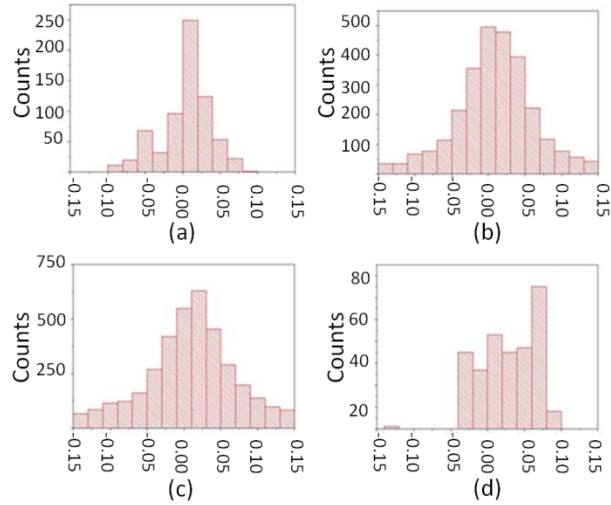


Figure 6. Dilatation strain for (a) untreated particles and particles annealed to (b) 100 °C, (c) 200 °C and (d) 300 °C.

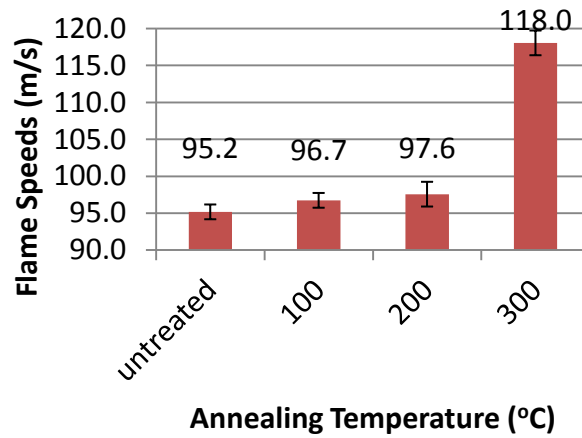


Figure 7. Flame speed as a function of annealing temperature. Average values for flame speed are reported above the bar and standard deviation in the measurements is also shown.



## Improving Aluminum Particle Reactivity by Annealing and Quenching Treatments: Synchrotron X-ray Diffraction Analysis of Strain

*Jena McCollum and Michelle Pantoya*

*Mechanical Engineering, Texas Tech University, Lubbock, TX 79409*

*Nobumichi Tamura*

*Advanced Light Source, Lawrence Berkeley National Laboratory, Berkeley, CA 94720*

**Table 1. Dilatational strain in Al particles, flame speeds when combined with CuO, and percent increase for all Al annealing temperatures. The average strain for the samples annealed to 100 and 200 °C are within the resolution of the machine, so their percent increase is negligible.**

Annealing Temperature (°C)	Average strain	% increase	Flame Speed (m/s)	% increase
<b>untreated</b>	1.00E-05	---	95.2	---
<b>100</b>	1.47E-05	---	96.7	---
<b>200</b>	1.53E-05	---	97.6	---
<b>300</b>	3.25E-05	660	118	24

